Absorption mechanisms in macroporous silicon photonic crystals

Daniel Segura García, David Cardador Maza, Jordi Llorca, Ángel Rodríguez Martínez, *Senior Member, IEEE*

***Abstract*—We investigate the origin of the large differences between the transmittance values obtained by numerical simulations and the ones experimentally obtained by FT-IR spectroscopy in macroporous silicon photonic crystals. To do so, previously reported data as well as new experimental measurements of macroporous silicon photonic crystal fabricated samples have been investigated by focusing on two possible causes of transmittance reduction: free carrier absorption and scattering. By means of simulations and experimental measurements, it has been proved that although *n*-doping in the bulk does not introduce meaningful losses, implanted ohmic contact imposes high absorption in the long wavelength region, ~40 % transmittance reduction. On the other hand, Lambertian light trapping as a consequence of light scattering by fabrication errors-deviations in the photonic crystals region, has been shown as a limiting mechanism for short wavelength absorption. The wavelength behavior of the Lambertian light trapping mechanism has evidenced a direct correlation with the used pitch. Indeed, it is caused by scatterers whose sizes are comparable with the modulation radius. This fact encourages continuing in the pitch reduction to further enhance the possibilities of this single etch, all silicon technology. By fabricating a swallow polished membrane, modulated ordered macroporous silicon technology can go beyond the 500 nm current limit without experiencing strong optical limitations imposed by bulk free carrier absorption or Lambertian light trapping.**

***Index Terms*—Macroporous silicon photonic crystals, electrochemical etching, silicon photonics, light scattering, optical losses.**

I. Introduction

MACROPOROUS silicon (MPS) photonic crystals (PhCs) have found application in different fields such as spectroscopic gas sensors [1] or narrowband selective thermal emitters [2]. However, one classical problem of MPS-PhCs has not been solved, the differences between theoretical simulations and experimental optical characterization of fabricated samples –see **Fig. 1**–. These differences can be mainly observed in the transmittance and the quality factor of the PhCs' optical response. Our group has previously reported the effect of absorption in the porous zone for samples with 2 µm horizontal period –pitch (*p*)– [3] and the consequences of the period deviations in the optical response [4]. Two main conclusions were drawn from these works. On the one hand we found that material absorption losses in the photonic crystal region were negligible for the measured samples. On the other hand, vertical period deviations result, mainly, in a significant bandgap reduction as well as a smoothing of the PhC optical response. However, this works are not able to explain the previously reported large differences in transmittance, and its wavelength dependence, between simulations and measurements [5]–[7]. As the reduction of periodicity is one of the future goals of MPS PhC technology, high absorption losses in short wavelengths could limit the development and establishment of this technology. For instance, low transmittance would reduce the dynamic range, and thus the sensitivity and the limit of detection, of spectroscopic sensors.

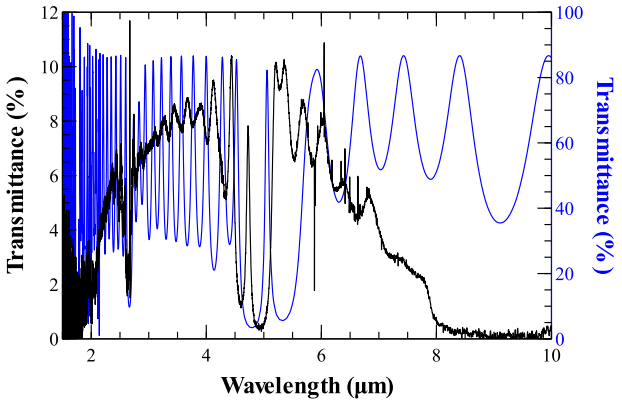

Fig. 1. Comparison between simulation (dashed blue line) and experimental measurement (solid black line) of the transmittance of a macroporous silicon photonic crystal with 700 nm pitch. FDTD simulations reveal much higher transmission than the experimental results. A clear wavelength dependence can be observed in the experimental measurements.

MPS-PhCs with 70-80 % maximum transmittance have been reported for $p \geq 2$ µm [3], [8]. In them, simulated and experimental results reasonably agree for wavelengths longer than those corresponding to the bandgap frequency, however, for shorter wavelengths, transmittance drops fast and the agreement between measurements and simulations is

This work was supported in part by the Spanish Commission of Science and Technology under Grant TEC2013-48147-C6-2-R, ENE2015-74009-JIN and RTI2018-093996, co-funded by the European Regional Development Fund.

D. Segura García, D. Cardador Maza, and A. Rodríguez Martínez are with the Department of Electronic Engineering, Universitat Politècnica de Catalunya, Barcelona 08034, Spain (e-mail: daniel.segura.garcia@upc.edu; david.cardador@upc.edu; angel.rodriguez@upc.edu).

Jordi Llorca with the Institute of Energy Technologies, Department of Chemical Engineering, and Barcelona Research Center in Multiscale Science and Engineering, Universitat Politècnica de Catalunya, Barcelona 08019, Spain (e-mail: jordi.llorca@upc.edu).

particularly poor. In the case of PhCs with smaller periodicity –p = 700 nm–, the reported transmittance values are far from FDTD simulations in the whole wavelength range [5]–[7], see Fig. 1**Error! No s'ha trobat l'origen de la referència.**. Furthermore, although there is a clear attenuation in the transmittance across the spectrum, the absorption losses impact is especially evident in wavelength regions above 6 µm and below 3.5 µm. In this article, we investigate different aspects which may have a direct impact in the MPS-PhCs' absorption. In this way, the extracted conclusions will help the understanding of MPS-PhCs and the future development of the technology.

II. METHODOLOGY

A. Experimental: fabrication and characterization

MPS-PhC samples have been fabricated and characterized in order to unveil the origin of the divergences between simulated and experimental results. They consist of 16 modulations –with 900 nm vertical period– with an embedded defect in the middle of the structure –120 nm radius and 2.5 µm long– and a 7 µm long tail to enhance the Q-factor [5]. One example can be seen in Fig. 2.

The fabrication of macroporous silicon PhCs was performed by photo-electrochemical etching (PEC). The details of the process can be found elsewhere [9]. The process starts with an *n*-type <100> crystalline silicon sample, single side polished in our case. The starting material has a resistivity close to 0.3 Ω cm due to the ~$3\cdot10^{16}$ cm^{-3} phosphorous doping. A N^+ layer is implanted on the backside –non polished side– to provide a low resistance transparent ohmic contact. The schematic of the doping distribution can be seen in Fig. 3. After, an inverted pyramid pattern following a square 700 nm pitch lattice distribution is transferred to the polished surface following the process of oxidation, lithography, reactive ion etching and, finally, TMAH anisotropic etching. The inverted pyramids act as nucleation centres where the pores start growing following the standard PEC [10]. In it, the profile of the pores is defined through the modulation of the back-side light intensity as well as the voltage applied to the sample. Membranes with different depths have also been performed through TMAH 25 % etching of the rear bulk silicon at 70 ºC.

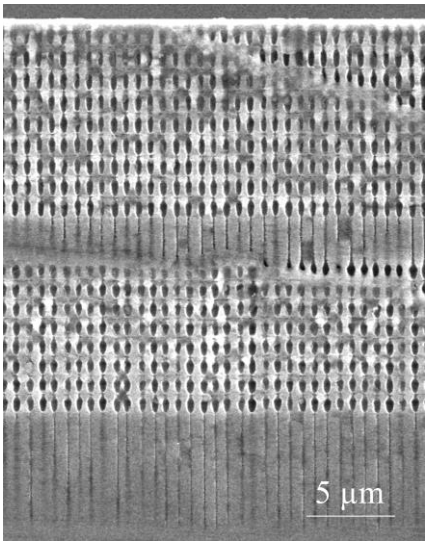

Fig. 2. SEM capture of the fabricated MPS-PhC.

The measurements of the optical transmittance have been made using a Fourier Transform Infrared Spectrometer (FT-IR), Bruker Vertex 70. The sample is located with the pores oriented in the light incidence direction. Two type of measurements have been done: direct transmission (DT)– measuring light traveling only at 0 degrees– and hemispherical transmission with a A562 model integrating sphere (HT) –measuring light scattered in all directions after the sample–. All measurements have been performed with a resolution of 4 cm^{-1} whereas the diameter aperture has changed depending on the type of measurement to maintain a good signal to noise ratio. For DT the aperture value has been 1 mm and for HT, 1.5 mm.

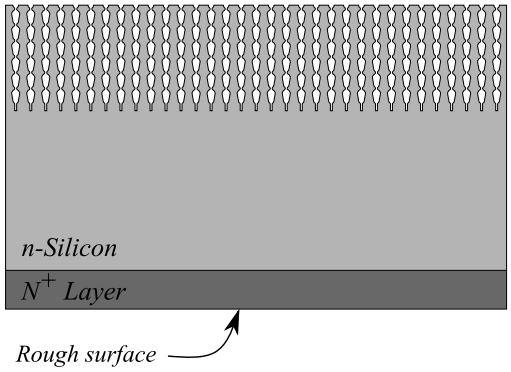

Fig. 3. Schematic plot of a macroporous silicon basic photonic crystal

B. Simulations

PhCs have been usually simulated with FDTD methods –see Fig. 1– with good results. Nevertheless, despite the high accuracy of the simulations, FDTD is a computational consuming method and, in our case, supposes an unacceptable limitation of time and resources when simulating large structures. In these cases, such as exploring the effects of silicon absorption in the bulk, TMM is the preferred method. TMM is a fast and relatively accurate method –1D approximation– which allows to simulate big samples. We

have created our own program to simulate the PhC, which has been defined as a stack of 20 nm 1D multilayers similarly to FDTD simulations [4], in this case, the "spherical" shape was defined as a set of 20 nm cylindrical slices. The average refractive index of each layer has been approximated considering the Maxwell-Garnett formula [11], [12]. In addition, experimental dispersive models [13] have been introduced to identify the effect of the losses in the bulk silicon.

III. Results and Discussion

The starting point to investigate the causes of the high absorption is the understanding of the role that substrates play. Two samples with no porous silicon patterns are measured in transmission: a <100> intrinsic crystalline silicon wafer and a *n*-type ~$3\cdot10^{16}$ cm^{-3} phosphorous doped crystalline silicon wafer with implanted N^+ back layer. Both samples are one side polished –see Fig. 3–. The measured transmittance spectra –both DT and HT– are plot in Fig. 4. In the intrinsic substrate the transmittance remains constant for HT measurement. This constant value can be theoretically obtained by multiplying the Fresnel coefficients for incident unpolarised 0 degrees' light at each of the two silicon/air interfaces, with a local transmission coefficient of 0.7 and a combined 0.49 transmission coefficient. But an important absorption is observed for short wavelengths in the DT case. This phenomenon comes from the unpolished side of the wafer, which scatters light in different directions, and it is dominant in short wavelengths [14]. By contrast, for long wavelengths, the transmittance tends to be the one measured with the integrating sphere.

In the case of the *n*-doped sample, it presents the opposite behaviour; transmittance is higher for shorter wavelengths than for the longer ones. In Fig. 4 we can see that for longer wavelengths there is an important transmittance reduction due to the free carrier absorption effect [15]. Smaller transmittance differences come from the different scattering in both sides of the wafers.

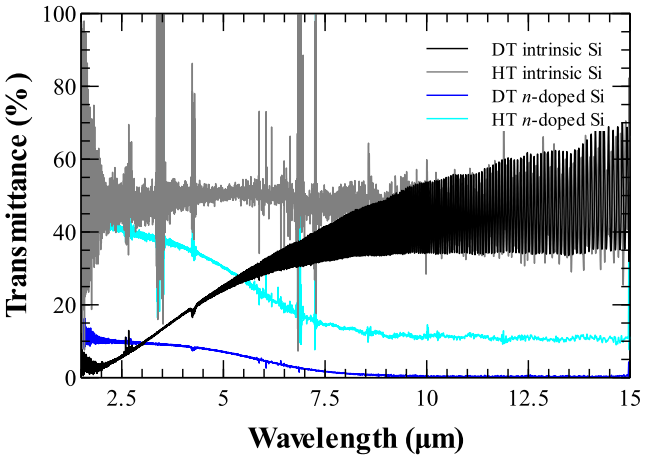

Fig. 4. Experimental measurements of intrinsic silicon wafer: DT (black), HT (grey); and *n*-type silicon wafer with implanted *N*+ back layer: DT (blue), HT (cyan).

A. Long wavelengths: effects of free carrier absorption

In Fig. 5(a) **Error! No s'ha trobat l'origen de la referència.**the absorption coefficient α, extracted from [13], can be observed for different silicon doping levels. It can be seen that absorption losses exponentially increase with the doping of the substrate. Schroder D.K. et al. [15] demonstrated that for longer wavelengths, the absorption coefficient increases following a quadratic relationship. They also proved that transmission losses due to free carrier absorption may be important in the range of resistivity below 20 Ω cm^{-2}.

To predict the optical impact that bulk silicon has in MPS PhCs, some simulations have been performed using TMM method. The absorption coefficients of Fig. 5(a) –and its wavelength dependence– have been introduced in the TMM simulations of the PhC, Fig. 5(b). Because our samples are single side polished, interference fringes produced by reflection in backside of the wafer are not observed in experimental measurements. For this reason, and to improve the visualization, TMM simulations have been smoothed to eliminate the interference fringes [16]. Although the approximation is good in the overall region, in the bandgap the smoothing of the response produces unreal high bandgap transmission and Q-factor reduction.

Fig. 5(b) shows that the bulk high doping may have an impact in the transmission of the PhC sample by increasing the absorption in the bulk. But based on the values from [17] and the simulations, a doping of $3\cdot10^{16}$ cm^{-3} –the one of our samples– should not result in a significant increase in absorption. Indeed, the transmission reduction that could be attributed to the bulk doping should be smaller than 2 %. The rule of thumb for the selection of the doping is that the doping of an appropriate substrate is obtained by multiplying the desired pore density given (in μm^2) by 10^{16} and take this number as doping density (in cm^{-3}) [10]. Roughly, this means that for MPS PhCs with pitch bigger than 500 nm, the doping level should be smaller than $4\cdot10^{16}$ cm^{-3} . For p > 500 nm no significant effect on transmittance, < 3 % decrease, should be associated with the doping of the substrate. For the possible smallest silicon macroporous periodicities [18], 50 nm < p < 300 nm, transmittance may become seriously affected, > 5 % drop. This is because doping follows a square ratio with pitch reduction and absorption coefficient exponentially grows with doping, rapidly increasing the absorption.

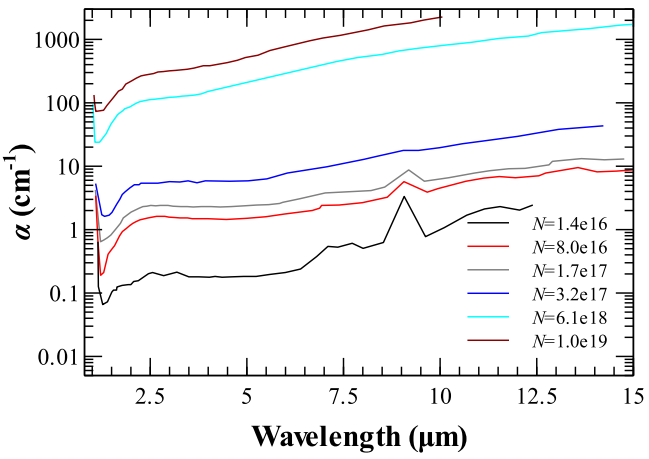

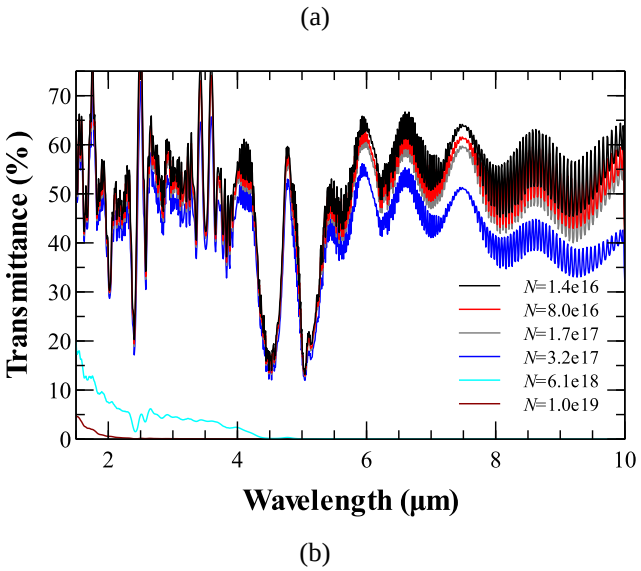

Fig. 5. (a) Absorption coefficient for different *n*-type doping levels of silicon. Data extracted from [13]. (b) TMM Simulation of the optical response of a PhC with bulk silicon applying the different absorption coefficients. In (b) the spectra have been smoothed to eliminate de fringes due to specular internal reflection in both sides of the simulated sample [16].

Even though the bulk silicon does not seem critical for our periodicity, the N^+ ohmic contact implanted in the back side of the wafer, although very thin –less than 5 µm–, may lead to significant absorption. To experimentally observe the effect of the bulk and the implanted N^+ layer in the PhCs' transmission spectra, a membrane with different etching depths has been performed on a sample. The results of the transmittance measurements, DT and HT, can be observed in Fig. 6(a) and Fig. 6(b) respectively. Different conclusions can be extracted from both of them. The N^+ implantation imposes high absorption. This absorption effect is evident in the increase in transmission in the case of the 35 µm etch after the removal of the N^+ layer. An increase from 8 % to 32 % appears in the near/mid infrared region and from 1.5 % to 50 % in the mid/long infrared region. Nevertheless, the high absorption introduced by N^+ implantation, which presents a clear inconvenient for the mid infrared (MIR) transmittance, could be used, along with the PhCs –which permits refractive index grading or resonant cavities–, to create long all silicon MIR absorbers [19] or all silicon selective absorbers [20]; a hot topic in recent years.

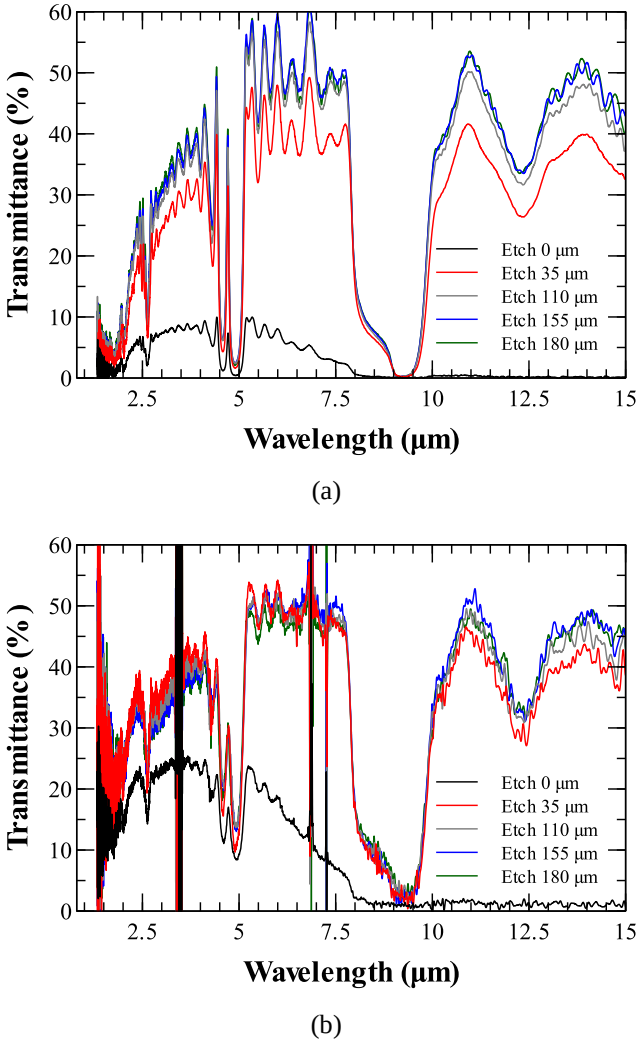

Fig. 6. Transmittance measurement of a macroporous silicon PhC with a membrane with different etching depths: (a) Direct transmittance, (b) Hemispherical transmittance.

After the N^+ layer is removed, the transmittance improvement for further membrane etching depths is irrelevant and could be attributed to deviations in the measurement point. Slightly more noticeable differences can be observed at longer wavelengths, as previously predicted by the absorption coefficient wavelength dependence.

There is a turning point in the transmittance in the bandgap wavelength region. The transmittance for longer wavelengths is similar to the one predicted in Fig. 5(b) for low doped substrates. However, for smaller wavelengths transmittance experiences a fast drop. A similar phenomenon can be observed in other previously reported data for longer pitches [3], [8]. In that case, the bandgap is centred at 20 µm and the transmittance begins to decrease at 17 µm, and eventually becomes practically null at the wavelength of 5 µm. This phenomenon cannot be attributed to the roughness of the sample's posterior surface, since, as we have seen in Fig. 4, with integrating sphere the transmittance at these wavelengths should be independent of the pitch and should tend to the MIR transmittance values.

B. Short wavelengths: effects of scattering and Lambertian light trapping

In macroporous silicon fabrication different undesired effects come along with the PEC process. Microporous silicon formed in the modulation walls, period deviations [21], wall roughness, spiking or branching conform a picture of the possible sources of error [22]. Microporous silicon, with a less than 2 nm pore width appears in the surface of the pores with similar dimension regardless of the periodicity. On the contrary, roughness in the modulation walls, period deviations, spiking and branching have similar sizes and are proportional to the modulation diameters. From the visual inspection of the samples, these sizes are estimated between 20 nm –0.03 *p*– to 200 nm –0.3 *p*– for a PhC with p = 700 nm.

As explained before, and by looking at Fig. 6 and at previous reported transmittance data for samples with $p \geq 2$ µm [3], [8], one can say that transmittance turning point –wavelength in which transmittance starts dropping– is related with the period/bandgap of the PhC. That is, about 5 µm for the case when p = 700 nm and about 17 µm when p = 2 µm. The low wavelength transmittance tendency, similar to the DT observed in Fig. 4 for intrinsic silicon, purports that scattering due to fabrication irregularities may be the cause.

In Fig. 7, DT and HT are compared for the 180 µm deep etch case. In this figure one can observe the ergodic/non-ergodic behaviour of the light inside the PhC sample. The light ergodic behaviour is understood as the behaviour of light rays in which a steady-state, temporally averaged, light-intensity distribution is identical with a statistical phase-space intensity distribution [23]. For wavelengths longer than the bandgap, the transmittance is stable and equal for DT and HT –see Fig. 7–. This means that for these wavelengths scattering is not significant; light travels through the sample and perpendicularly escapes, in a system which behaves non-ergodically. In the case of shorter wavelengths, the system fast turns to exhibit an ergodic behaviour, light is randomly scattered in the photonic crystal region and the temporally averaged light intensity distribution inside the bulk silicon will tend to be the refractive index square times the incident light intensity [23]. Thus, light inside the PhC/bulk loses all external incidence angle memory after firsts scattering events, and the angular randomization tends to be the rule [23]. Indeed, it can be observed that the transmission is still the same for DT than for HT, indicating that scattered light cannot escape from the sample, whose escape cone solid angle –obtained from Snell's law– is $\Omega_c \approx 16$ deg. Therefore, the system becomes a Lambertian trapping system.

In Fig. 7, when 3 µm < λ < 5 µm the PhC behaves as a Lambertian scatterer whereas the "rough" bottom of the sample behaves as a specular reflector. When the wavelength is sufficiently short, λ < 3 µm, the photons "see" the irregularities of the bottom surface and DT and HT start to differ. This is because the bottom of the sample also scatters light and Lambertian reflexion/transmission appear. DT still measures the light that passes through the sample without scattering, however, in HT part of the non-perpendicularly scattered light is measured, increasing the transmittance as a result.

The TMAH etching employed to fabricate the membrane reduces the roughness of the sample bottom [24], which in turns, reduces the wavelength in which the bottom side of the wafer starts to effectively scatter light. This can be seen in Fig. 6(b), for samples that have been strongly etched with TMAH, DT is equal to HT. However, for the 30 µm etching depth case, a difference of approximately 10 % is observed between DT and HT measurements. In this case, the rear side of the sample may still present significant roughness.

Although wavelengths shorter than the bandgap ones may seem useless, they are not. Apart from the main bandgap, secondary bandgaps and/or smaller periodicities could dote photonic crystals of further features that cannot be profited at the moment due to the strong scattering. In our case this is an drawback, however, Lambertian trapping with porous silicon have found applications for light trapping in solar cells [25].

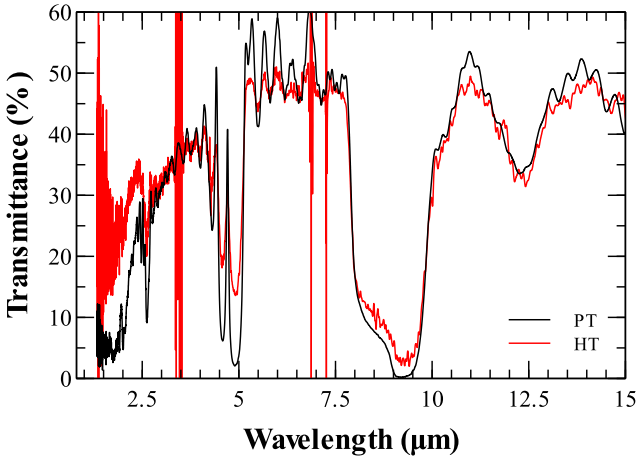

Fig. 7. Comparative between HT and DT for a 180 µm etched membrane.

Another consequence of the angular randomization produced by scattering appears in the main bandgap –with its peak–. When a perpendicularly incoming photon, $k_\perp = 0$, is scattered due to an irregularity in the medium, its direction is modified. The photon, with its new k, $k_{new} \neq k_\perp \neq 0$, does not experience the same PhC band structure as the $k_\perp$ one and it is likely that the PhC will become almost transparent for it [26]. This can be seen in the bandgap transmission of Fig. 7. In the HT case, the photons which have been scattered either do not see the bandgap or easily scape from the cavity, leading to higher bandgap transmission –they have not experienced the destructive interferences that conform the bandgap–. Due to the same reason, the lifetime of the photon inside the cavity is reduced, and as a consequence the Q-factor is reduced, similarly to what happens in 1D nanoporous material PhC with microcavity [26]. When measuring DT, only photons travelling in the incoming direction are measured. These photons have either not been scattered or have been scattered in the incoming perpendicular direction. Hence, all of them have experienced the same forbidden band, increasing the photon lifetime inside the cavity and experiencing the bandgap in the ideally designed direction. As a result, better quality factors and lower bandgap transmission are obtained for DT. This is a reason which suggests that in commercial

applications, DT should be used to obtain optimum designs, for example in gas sensors.

To understand the causes of scattering, the theoretical reduction of light transmittance due to Mie scatterers in a non-absorbing medium, have been compared with experimental absorbance results. This allows us to estimate the theoretical scatterers size –or, equivalently, their scattering cross section– and from there, infer a qualitative description of the causes of scattering.

The experimental absorbance is considered:

$$A(\%) = \frac{T_0 - T}{T_0} 100 \qquad (1)$$

where T is the FT-IR measured direct transmittance. T_0 is the transmittance experimentally obtained for a bare silicon wafer –see Fig. 4–, which takes a constant value of approximately 49 %. This value, as explained before, can also be theoretically obtained using Fresnel equations for 0 degrees incident unpolarised light in the two silicon/air interfaces. Despite the PhC modifies the distribution of energy by introducing peaks and dips in the spectrum, when the PhC influence is reduced –outside the bandgap– and according to energy conservation theory, the transmittance tends to this value –see 5 to 7.5 μm wavelength region in Fig. 7–.

On the other hand, the simulated absorbance due to scattering can be described as [25], [27]:

$$A = \frac{\sigma_{sca} l N}{\ln 10} = \frac{\sigma_{sca} l \, P_{sca} / \upsilon}{\ln 10} \qquad (2)$$

Where σ_{sca} is the scattering cross section and l is the path length –the PhC's size in this case, 25 μm approx.–. N is the volume density of scatterers, which can be obtained by dividing the porosity of the material due to the scatterers, P_{sca}, by the scatterer's volume, υ, [25]. The absorption cross section is obtained from Mie theory, approaching the irregular shapes of the real scatterers to non-absorbing spheres with different diameters. Effective medium theory is considered in the calculation due to the porous nature of the material and the studied wavelength, with an average refractive index $n_{eff} \approx 2.93$, from model [4].

Restrictions to the size of the scatterers are introduced from visual inspection –see Fig. 2– and from radius/period deviation available data [4]. Therefore, the scatterer's diameter, d_{sca}, is expected to be smaller than half of the pore radius. In our case, this means that the scatterers should have a diameter smaller than 100 nm. In fact, standard deviations for periods and radius are approximately 60 nm and 20 nm, respectively [4].

The porosity of the PhC due to the desired pores –not including the defects in fabrication– can be found around 30 % [3]. Because all the described scattering mechanisms occur close to the pore walls –F^- ions cannot etch silicon that is not in contact with the surface–, and according to SEM images, we consider that the porosity due to the scatterers should be similar to ideal porosity, $P_{sca} \approx P \approx 30$ %.

Both experimental and simulated absorbance can be seen in Fig. 8 for P_{sca} = 30 % and different σ_{sca}. In this figure one can see that small perturbations, with diameters below 40 nm –in which we include the microporous formatted at the walls of the porous–, do not introduce meaningful losses. Therefore, as expected by the pitch dependency on the scattering, the microporous silicon formation at the walls of the modulations will not be the cause of Lambertian light trapping, at least for the studied wavelengths. On the contrary, we can say that the main cause of the short wavelength absorption is the scattering produced by scatterers with diameters above 40 nm –$d_{sca} \approx 0.06\,p$–. Perturbations with diameter $d_{sca} > 0.28\,p$ –200 nm– would lead to excessive scattering, which we do not see in our measurements. Summing up, defects with size $0.28p < d_{sca} < 0.06\,p$ are the dominant source of scattering, and as a consequence of absorption, at wavelengths shorter than the bandgap.

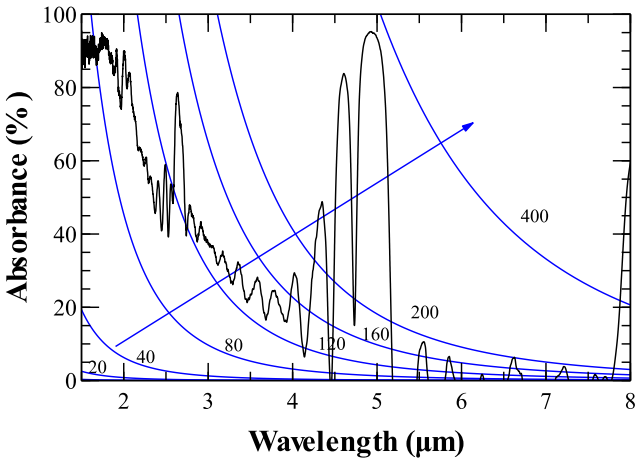

Fig. 8. Comparative of experimental DT absorbance (black) and theoretical DT absorbance for P_{sca} = 30 % and different σ_{sca} (blue).

Although some improvements in the fabrication process can be introduced, better control of the period dispersions or spiking reduction through profile currents correction, the correction of this non-idealities have difficult solution. Thus, due to the scattering dependence on period, to work in smaller wavelengths the pitch will have to be reduced. Another improvement could be the use of high temperature argon annealing of MPS [28]. In this process the silicon reorganization and conversion to multilayer silicon-air structure could importantly reduce the size and density of the scatterers.

IV. Conclusion

High losses have been a limiting factor for the use of photonic crystals in real applications. In this work we have observed that the high absorbance values are mainly explained by two phenomena: free carrier absorption and scattering Lambertian light trapping.

Free carrier absorption in the *n*-doped bulk silicon has not proved to be a critical aspect for periods of more than 300 nm, the attributable losses due to this are smaller than 2 %. However, the implanted ohmic contact does introduce high absorbance, almost a 40 % transmittance reduction. Hence, a

rear etching to remove this N^+ doped layer will rapidly boost the transmission, especially in the long wavelength region, less affected by scattering. There is no need of performing deep etches because scattering will always be present and the transmittance will only slightly increase for deeper etches. The rear TMAH etching can also be profited to increase the smoothness of the wafer's backside, reducing the effect of the scattering in this surface.

Lambertian light trapping produced by the scattering in the PhC region has been the main absorption enhancement mechanism for wavelengths below the bandgap. It has been deduced that scattering is not importantly affected by small perturbations such as the one produced by the microporous silicon produced at the walls of the modulations. However, defects which depend on the period, such as radius-period deviations, branching or spiking, which are bigger when longer periods are used, cause the system to behave ergodically. As a result, angular randomization and light trapping tend be the rule, inducing an absorption increase for wavelengths shorter than the bandgap ones.

REFERENCES

[1] Cardador Maza, David; Segura Garcia, Daniel; Deriziotis, Ioannis; Llorca, Jordi; Rodriguez Martinez, "Macroporous silicon filters, a versatile platform for NDIR spectroscopic gas sensing in the MIR," unpublished.

[2] Cardador Maza, David; Segura Garcia, Daniel; Deriziotis, Ioannis; Garín, Moisés; Llorca, Jordi; Rodriguez Martinez, "Empirical demonstration of CO2 detection using thermally tuneable macroporous silicon photonic crystals as selective thermal emitters," unpublished .

[3] D. Vega, D. Cardador Maza, T. Trifonov, M. Garin Escriva, and A. Rodriquez Martinez, "The Effect of Absorption Losses on the Optical Behaviour of Macroporous Silicon Photonic Crystal Selective Filters," *J. Light. Technol.*, vol. 34, no. 4, pp. 1–1, 2015.

[4] D. Segura, D. Vega, D. Cardador, and A. Rodriguez, "Effect of fabrication tolerances in macroporous silicon photonic crystals," *Sensors Actuators, A Phys.*, vol. 264, 2017.

[5] D. Cardador, D. Vega, D. Segura, T. Trifonov, and A. Rodríguez, "Enhanced geometries of macroporous silicon photonic crystals for optical gas sensing applications," *Photonics Nanostructures - Fundam. Appl.*, 2017.

[6] D. Cardador, D. Segura, and A. Rodríguez, "Photonic molecules for improving the optical response of macroporous silicon photonic crystals for gas sensing purposes," *Opt. Express*, vol. 26, no. 4, 2018.

[7] D. Cardador, D. Segura, D. Vega, and A. Rodriguez, "Improved transmission and thermal emission in macroporous silicon photonic crystals with 700 nm pitch," in *2017 Spanish Conference on Electron Devices, CDE 2017*, 2017.

[8] D. Vega, J. Reina, and A. Rodriguez, "Macroporous silicon photonic crystals for gas sensing," in *2013 Spanish Conference on Electron Devices*, 2013, pp. 143–146.

[9] V. Lehmann, "The physics of macroporous silicon formation," *Thin Solid Films*, vol. 255, no. 1–2, pp. 1–4, Jan. 1995.

[10] V. Lehmann, *The electrochemistry of silicon : instrumentation, science, materials and applications*. Wiley-VCH, 2002.

[11] J. Schilling, F. Müller, R. B. Wehrspohn, U. Gösele, and K. Busch, "Dispersion relation of 3D photonic crystals based on macroporous silicon," *MRS Proc.*, vol. 722, p. L6.8, Feb. 2002.

[12] M. Garín, T. Trifonov, A. Rodríguez, L. F. Marsal, and R. Alcubilla, "Optical properties of 3D macroporous silicon structures," *Mater. Sci. Eng. B Solid-State Mater. Adv. Technol.*, vol. 149, no. 3, pp. 275–280, 2008.

[13] D. Chandler-Horowitz and P. M. Amirtharaj, "High-accuracy, midinfrared (450cm−1⩽ω⩽4000cm−1) refractive index values of silicon," *J. Appl. Phys.*, vol. 97, no. 12, p. 123526, Jun. 2005.

[14] S. Hava, J. Ivri, and M. Auslender, "Wavenumber-modulated patterns of transmission through one- and two-dimensional gratings on a silicon substrate," *J. Opt. A Pure Appl. Opt.*, vol. 3, no. 6, pp. S190–S195, Nov. 2001.

[15] D. K. Schroder, R. N. Thomas, and J. C. Swartz, "Free Carrier Absorption in Silicon," *IEEE J. Solid-State Circuits*, vol. 13, no. 1, pp. 180–187, Feb. 1978.

[16] J. R. Ferraro and K. Krishnan, *Practical Fourier transform infrared spectroscopy : industrial and laboratory chemical analysis*. Academic Press, 1990.

[17] W. Spitzer and H. Y. Fan, "Infrared Absorption in n -Type Silicon," *Phys. Rev.*, vol. 108, no. 2, pp. 268–271, Oct. 1957.

[18] V. Lehmann and U. Grüning, "The limits of macropore array fabrication," *Thin Solid Films*, vol. 297, no. 1–2, pp. 13–17, Apr. 1997.

[19] K. Gorgulu, A. Gok, M. Yilmaz, K. Topalli, N. Bıyıklı, and A. K. Okyay, "All-Silicon Ultra-Broadband Infrared Light Absorbers," *Sci. Rep.*, vol. 6, no. 1, p. 38589, Dec. 2016.

[20] M. Desouky, A. M. Mahmoud, and M. A. Swillam, "Silicon based mid-IR super absorber using hyperbolic metamaterial," *Sci. Rep.*, vol. 8, no. 1, p. 2036, Dec. 2018.

[21] A. F. Koenderink, A. Lagendijk, and W. L. Vos, "Optical extinction due to intrinsic structural variations of photonic crystals," *Phys. Rev. B*, vol. 72, no. 15, p. 153102, Oct. 2005.

[22] V. Lehmann, *The electrochemistry of silicon : instrumentation, science, materials and applications*. Wiley-VCH, 2002.

[23] E. Yablonovitch, "Statistical ray optics," *J. Opt. Soc. Am.*, vol. 72, no. 7, p. 899, Jul. 1982.

[24] K. Sakaino and S. Adachi, "Study of Si(1 0 0) surfaces etched in TMAH solution," *Sensors Actuators A Phys.*, vol. 88, no. 1, pp. 71–78, Jan. 2001.

[25] H. Seel and R. Brendel, "Optical absorption in crystalline Si films containing spherical voids for internal light scattering," *Thin Solid Films*, vol. 451–452, pp. 608–611, Mar. 2004.

[26] M. Toledo Solano, Y. G. Rubo, J. A. del Río, and M. C. Arenas, "Rayleigh scattering in multilayered structures of porous silicon," *Phys. status solidi*, vol. 2, no. 10, pp. 3544–3547, Aug. 2005.

[27] M. R. Rashidian Vaziri, A. Omidvar, B. Jaleh, and N. Partovi Shabestari, "Investigating the extrinsic size effect of palladium and gold spherical nanoparticles," *Opt. Mater. (Amst).*, vol. 64, pp. 413–420, Feb. 2017.

[28] M. Garín, C. Jin, D. Cardador, T. Trifonov, and R. Alcubilla, "Controlling Plateau-Rayleigh instabilities during the reorganization of silicon macropores in the Silicon Millefeuille process," *Sci. Rep.*, vol. 7, no. 1, p. 7233, Dec. 2017.

Daniel Segura García received the B.S degree in industrial electronics from the Universitat Politècnica de València, València, Spain, in 2012, and the M.S. degree in electronic engineering from the Universitat Politecnica de Catalunya, Barcelona, in 2015. He is currently working toward the Ph.D. degree in electronic engineering. His research interests include macroporous silicon, integrated silicon photonics, photonic crystals, and biochemical spectroscopic sensors.

David Cardador Maza received the B.S degree in physics from the Universitat de Barcelona, Barcelona, Spain, in 2008, and the M.S. degree in electronic engineering from the Universitat Politècnica de Catalunya, Barcelona, in 2013. He is currently working toward the Ph.D. degree in electronic engineering. His research interests include macroporous silicon, photonic crystals, and photovoltaic systems.

Jordi Llorca received the PhD degree in chemistry from the Universitat de Barcelona, where he was later appointed Associate Professor and Ramon y Cajal Fellow. In 2005 he joined the Universitat Politècnica de Catalunya and in 2014 he became Full Professor as Serra Húnter Fellow. He received the ICREA Acadmia Award in 2009 and in 2014. He is working with photocatalysts with semiconductors, metal nanoparticles and photonic crystals for energy and environmental applications.

Ángel Rodríguez Martínez (M'92–SM'08) received the B.S. degree in telecommunication engineering from the Universitat Politècnica de Catalunya, Barcelona, Spain, in 1987 and the Ph.D. degree in electronic engineering from Interuniversity Microelectronics Centre, Belgium, in 1992. He became an Associate Professor with the Escuela Técnica Superior de Ingenieros de Telecomunicación de Barcelona in 1993. He has worked in solar cells, polysilicon TFTs, ´ and MEMS devices. His current research topics include bio-sensors, macroporous silicon, and photonic crystals